*Fibers and Polymers* 2015, Vol.16, No.2, 276-284
DOI 10.1007/s12221-015-0276-6

ISSN 1229-9197 (print version)
ISSN 1875-0052 (electronic version)

# Nanosized Carbamoylethylated Cellulose as Novel Precursor for Preparation of Metal Nanoparticles

**A. Hebeish, S. Farag, S. Sharaf, and Th. I. Shaheen***

*Textile Research Division, National Research Centre, Cairo 12311, Egypt*
(Received July 1, 2014; Revised September 12, 2014; Accepted September 19, 2014)

**Abstract:** Current work has three-fold objective: (a) to augment the dispersability of cellulose nanowhiskers (CNW) through carbamoylethylation; (b) to make use of nano-carbamoylethyl cellulose (NCEC) as precursors for preparation of metal nanoparticles and, (c) to apply the so obtained metal nanoparticles in production of smart conductive textiles. To achieve the goal, CNW was reacted with acrylamide to yield NCEC having D.S. of 0.8 and a size of *ca* 37 nm. NCEC is more thermally stable than CNW. NCEC lost completely its crystalline structure, that is, NCEC is a polymeric material without crystalline domains. Beside its solubility in water and its polymeric nature, NCEC bears terminal carbamoylethyl and carboxyethyl groups along with its cellulosic backbone. These properties would advocate NCEC to function a dual role: reducing and stabilizing agent during the synthesis of metal nanoparticles. Silver nanoparticles (AgNPs) were produced in spherical shape with small sizes as signified by UV-vis spectroscopy and Transmission Electron Microscopy (TEM) with extremely high stability upto concentration as high as 2000 ppm. Therefore, AgNPs was employed successfully as highly functional, effective and adequate precursor for synthesis of smart conductive fabrics.

**Keywords:** Nanosized carbamoylethyl cellulose, Cellulose nanowhiskers, Silver nanoparticles, Conductive textiles

## Introduction

At present, much attention is given to the development of effective green materials from renewable sources which are biodegradable and non-toxic to humans and environment [1-5]. Cellulose is by far a biopolymer offering these advantages. Equally interesting is the use of stiff nanometric particles for reinforcement in polymeric matrixes, composites and nanocomposites processing. These nanometric materials are exemplified by cellulose nanocrystals. According to the literature, cellulose nanocrystals are also whiskers, nanofibers, cellulose crystallites or crystals. They represent the crystalline domains in supermolecular structure of cellulosic fibers. Isolation of these domains is induced by acid hydrolysis. In this way the crystalline domains are called as per their physical characteristics including stiffness, thickness, and length [3].

Cellulose whiskers are defined by De Souza Lima *et al.* and Samir *et al*. [6-8] as regions growing under controlled conditions, and, in so doing, they allow individual high-purity crystals to form. Due to their high mechanical properties and renewable nature, compliment of cellulose nanowhiskers (CNW) as reinforcing filler in synthesis of polymer nano-composites has become great interest [9,10]. However, CNW particles are difficult to disperse in solvents and easily from aggregates during drying as a manifestation of plenty of hydroxyl groups that are present on the surface of CNW. This defect restricts the applications of CNW. That is why different approaches have been undertaken to improve the dispersability of CNW by, for example, the addition of surfactants [11] and modification by surface grafting or etherification [12,13]. Cellulose contains 31.48 % by weight of hydroxyl groups (one primary and two secondary per anhydroglucose unit) (AGU). Accessibility of these cellulose hydroxyls presents enormous opportunities for preparing useful cellulose derivatives. Reactivity of the hydroxyl groups of cellulose varies according to the reaction medium in which functionalization is done. For example, the order of reactivity for etherification performed in an alkaline medium is 2>6>3 while the primary hydroxyl group (OH-6) is the most active in esterification [14].

Particularly notable nowadays are the great deal of research and technical work which are directed towards synthesis and characterization of metal nanoparticles in order to exploit their useful properties such as good electrical conductivity and antimicrobial activity as well as cost-effective [15-18]. There are also several reports on the use of cellulose nanoparticles as a stabilizing matrix for Ag, Au, Ni, Pt, Pd and $TiO_2$ nanoparticles [19-24] according to various methods [25]. The applications encompass, interalia, the production of textiles with new properties such as conductivity which is rather a new field being investigated [26]. In fact, CNW has been prepared as per sulfuric acid hydrolysis by our group [27]. Recently, our study is extended to accentuate the dispersability of CNW by modification of CNW via graft copolymerization with polyacrylamide in order to modify surface performance [28].

Current study is undertaken with a view to development a new precursor through carbamoylethylation of CNW; and to study the properties of thus synthesized nano-sized carbamoylethyl cellulose; as well as, to harness the nano-sized carbamoylethyl whiskers as a precursors for preparation of silver nanoparticles; and finally, to utilize the so obtained silver nanoparticles in the synthesis of smart conductive

*Corresponding author: Shaheen_chem@yahoo.com

textile products. To our knowledge, this is a first paper dealing with modification of CNW through carbamoylethylation process.

## Experimental

### Materials

Cotton sliver, Giza 86 was supplied by Cotton Research Institute, Giza. Sodium hydroxide, sulfuric acid (95-98 %), acrylamide and $AgNO_3$ (Fluka) were all of laboratory grade chemicals.

### Methods

***Preparation of CNW***

CNW were prepared from purified and bleached cotton sliver using 60 % (w/w) sulfuric acid for 60 min at 60 °C as described in previous work [27].

***Carbamoylethylation of CNW***

5 g of freshly prepared CNW and 1.0 g·mole$^{-1}$ NaOH were mixed thoroughly for 5 min in a stainless steel cup using mechanical stirrer at room temperature. The latter was raised by heat of this treatment and, therefore, the cup was left to cool down to room temperature. 0.07 mole/*l* acrylamide was dissolved in 3 m*l* distilled water with good mixing followed by 3 m*l* of isopropanol and mixed thoroughly for 5 min. At this end, the mixture was added to the CNW/NaOH prepared as outlined blow. Thus obtained mixture was transferred into a stoppered flask and kept for 120 min at 60 °C in a thermostatic water bath. At the end of reaction time, the product was neutralized with an acetic acid/ethanol mix. (1/20, v/v) and followed by soxhlet extraction with ethanol/water mix. (80:20) for purification and, finally dried at 60 °C.

***Preparation of Silver Nanoparticles (AgNPs)***

The resultant namely nano-size carbamoylethyl cellulose (NCEC) was used as a precursor for preparation of silver nanoparticles. 1.0 g NCEC was dissolved in little amount of distilled water under vigorous stirring, followed by, addition of 0.3 g NaOH to the solution. After a while, the solution was completed to 100 m*l* and then temperature was raised to about 70 °C. To this solution, $AgNO_3$ at different concentrations was added drop-wise under stirring for 30 min. The reaction solution was observed to change from colorless to yellow and then brown. The reduction of silver ions was, routinely, monitored by visual inspection of the solution as well as by UV-vis spectra, and transmission electron microscopy (TEM).

***Loading of Silver Nanoparticles onto Cotton Fabrics***

Cotton fabric with a dimension of 15 cm×15 cm was soaked in 100 m*l* of silver colloidal solution for 1 min then squeezed to 100 % wet pick up using laboratory padder. This was followed by drying the so padded sample at 60 °C for 90 min.

### Analysis and Characterization

The amide content (m.eq-$CONH_2$/100 g sample) was calculated from the nitrogen content which was determined according to the micro Kjldahl method [29]. The carboxylic content (m.eq-COOH/100 g sample) of the prepared NCEC samples was determined using the alkalimetric method [30].

The total ether content=
the amide content+the carboxylic content

The degree of substitution (D.S.) of nano-sized carbamoylethyl cellulose (NCEC) sample was calculated as follows [31]:

$$\text{D.S.} = \frac{(0.162)\times(\text{ether content})}{100-(0.071)\times(\text{ether content})}$$

The nano-sized carbamoylethyl cellulose (NCEC) was also characterized using fourier transform infrared spectroscopy (FTIR) (S-100 FT-IR spectrometer, Perkin Elmer, USA) to verify the structure of NCEC. Further, the degrees of crystallinity of the NCEC is measured by X-ray diffraction (XRD) using D500 diffractometer (SIEMENS) operated at 30 kV and 15 mA. For studying the size and size dispersion of the NCEC, UV-vis spectroscopy (T80-V 5.5), transmission electron microscopy (TEM) (JEOL 1200, JEOL USA, Inc.) and dynamic light scattering (DLS) (Zeta sizer nano series (Nano ZS), Malvern, UK) were employed. Also, the thermal gravimetric analysis (TGA) was undertaken using TGA/SDT Q600 analyzer. Scanning electron microscopy (SEM) image for fabrics loaded with metal nanoparticles was obtained with JSM-5400 instrument (Jeol, Japan). electron probe microanalyser, which is equipped with energy disperse X-ray spectroscopy (EDX) for chemical composition analysis. The electrical conductivity of the dried metal-fabrics composite was determined at ambient room temperature (25 °C) using a Hewlett Packard 6634B System DC Power Supply and a digital Hewlett Packard 34401A Multimeter.

## Results and Discussion

### Synthesis of Nano-sized Carbamoylethyl Cellulose Whiskers (NCEC)

Generally, vinyl monomers can be grafted onto cellulose by graft copolymerization through various methods. However, there are vinyl monomers such a, acrylonitrile and acrylamide that serve as etherifying agent and reacts with cellulose in an alkaline medium [32].

CNW with size diameter ranging from 10-25 nm and length ranges from 80-200 nm has been prepared from cotton sliver using 60 % (w/w) $H_2SO_4$ for 60 min at 60 °C [27]. Acrylamide can be reacted via addition reaction with cellulose nanowhiskers to form carbamoylethyl ether of cellulose nanoparticles according to Michael addition as represented in Scheme 1. The latter illustrates the etherification of CNWwith acrylamide in presence of alkali. In this regard, it is probable that a side reaction occurs in which the acylamino group can be saponified to carboxyl group. Indeed carboxyethyl cellulose is inevitably formed when the

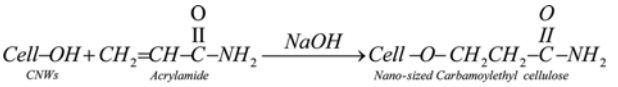


Side Reaction

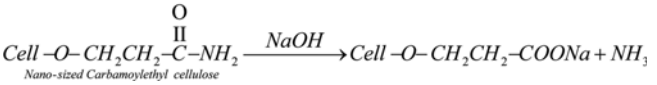


**Scheme 1.** The etherificaition of CNW with acrylamide in alkaline semi-dry process.

carbamoylethylation reaction is conducted in a higher alkaline aqueous medium at elevated temperature [33].

Nitrogen content and carboxyl content of NCEC were determined and taken as measures for the extent of carbamoylethylation and the carboxyethyl groups inevitably formed, respectively. Results obtained indicated that NCEC exhibits 2.4 % amide content which is equal to *ca* 200 m.eq-$CONH_2$/100 g sample. Meanwhile caboxyl content (COOH) reaches a value of 156.25 m.eq-COOH/100 g sample. This means from these data that the total ether content is 356.25 m.eq/100 g sample. Moreover, the D.S. of the so-prepared NCEC is 0.8 indicating that 26.7 % of the CNW hydroxyls are etherified and 73.3 % are still free. It is as well to emphasize that, D.S. 0.8 is directly responsible for solubilization of nanosized carbamoyl cellulose whiskers (NCEC) in distilled water to attain a clear solution.

## Characterization of NCEC

### *FT-IR*

Figure 1 shows the FTIR of CNW and the nanosized carbamoyl cellulose whiskers derived therof (NCEC). NCEC has a wide band 3000-3700 $cm^{-1}$ for the stretching frequency of the -OH and -NH groups, which become stronger than the band of the stretching vibration of -OH of the native cellulose. The broadening of this band indicates presence of many numbers of hydroxyl groups and the existence of intramolecular hydrogen bonding. Comparing the spectra of CNW and NCEC, FTIR spectra of the latter provides evidence of etherification by an increment in the intensity of the major ether bands at 1056 $cm^{-1}$. Further, the newest peaks at 1660 and 1450 $cm^{-1}$ for the NCEC are assigned to amide I (C=O stretching) and amide II (C-N stretching) bands, respectively. Furthermore, presence of another two strong new peaks at 1567 and 1424 $cm^{-1}$ are attributed to the asymmetrical and symmetrical stretching of $-COO^-$ groups, respectively. Those new peaks confirm the introduction of $CH_2$-$CH_2CONH_2$ moieties onto the molecular structure of cellulose nanowhiskers via etherification reaction. The additional carboxyl groups shown in spectrum above was an assignment for the occurrence of a saponification reaction.

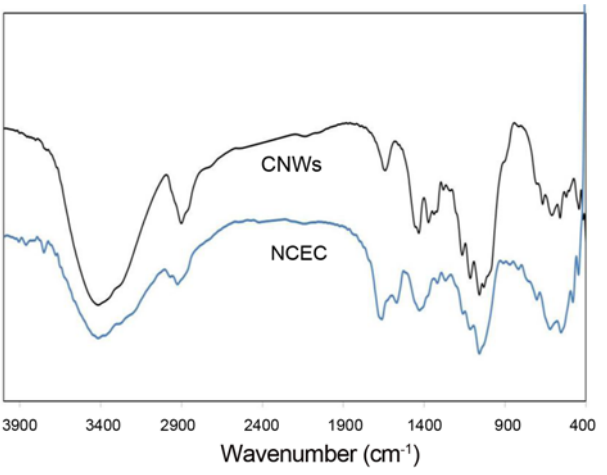


**Figure 1.** FT-IR spectra of CNW and NCEC.

### *XRD Analysis*

The XRD patterns of CNW and its derivative NCEC are shown in Figure 2. It is seen that, the crystallographic form CNW obeys cellulose I structure. CNW represents the principal peaks at $2\theta$ values 14°, 16°, 22°, and 35°. These four peaks correlate, respectively, with [101], $[101]^-$, [200] and [400] crystal lattice planes [34,35]. While the diffraction curve of NCEC represents two strong and characteristic peaks at $2\theta$ values 22° and 35° indicating total loss of crystallinity structure of cellulose derivative as also calculated from crystallinity index calculation [36].

As a direct consequence of the aforementioned results it is evident that carbamoylethylation of CNW diminishes the crystallinity of the parent CNW. This may be attributed to the direct contact of NaOH with CNW in almost dry state, which causes swelling of nanowhiskers followed by redistribution of internal hydrogen bonds [37].

### *TEM*

Figure 3 shows the TEM images of NCEC and CNW. It seems from Figure 3 that the rod-like shape of CNW

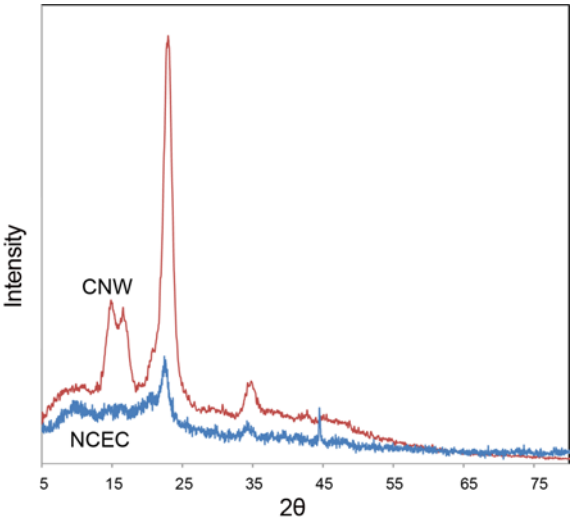


**Figure 2.** XRD patterns of CNW and NCEC.

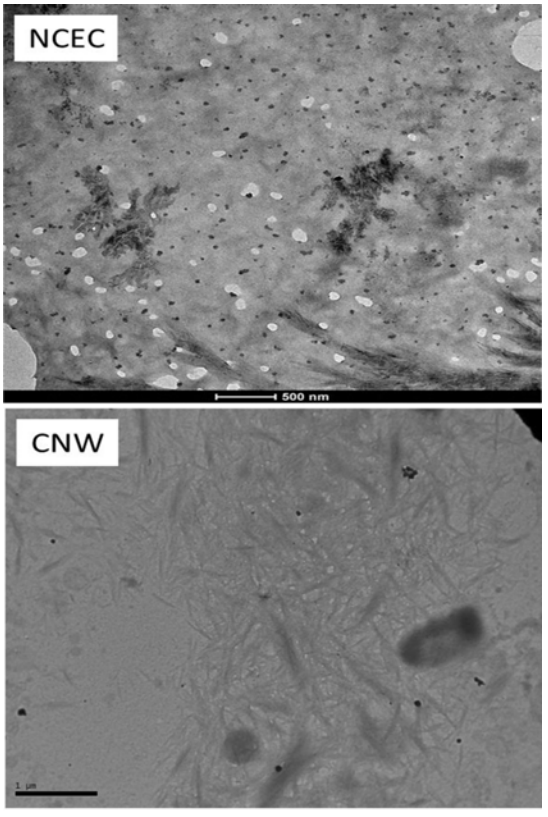


**Figure 3.** TEM of NCEC and CNW.

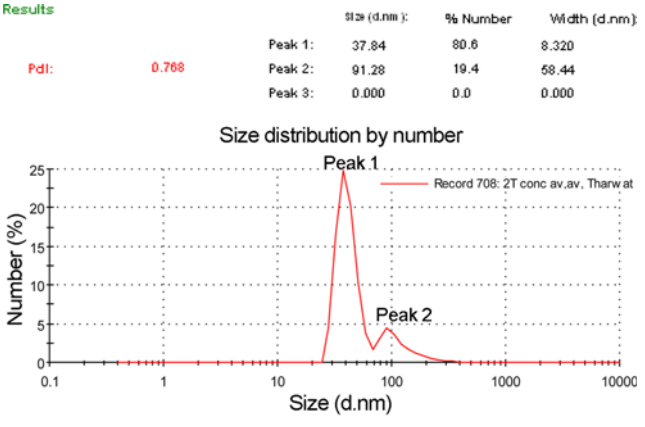


**Figure 4.** Dynamic light scattering showing size and size distribution of NCEC.

disappears and NCEC exhibits an approximately ball-like structure and disperses homogeneously on the copper grid. This result emphasizes that the crystallinty of CNW was devastated after occurrence carbamoylethylation; a point which indicates the formation of a newly synthezied carbamoylethyl cellulose on the amourphous form of CNW. The results are in good agreement with those obtained from XRD analysis given below.

Figure 4 shows the size and size distribution of NCEC which were characterized as per the dynamic light scattering (DLS) technique. Based on this figure, it can be concluded that the average particle size of NCEC is 37.84 nm with a majority of 80.6 % (Peak 1). However, there are some aggregates in a size range of 91.28 nm with small portion of 19.4 % (Peak 2). Hence, Figure 4 clarifies that NCEC is a well-dispersed polymer with size majority of 37.84 nm.

***TGA***

Figure 5 shows the thermo gravimetric analysis of CNW and NCEC. The results are also represented in Table 1. Basically, the loss of weight at 100 °C is due to the loss of water naturally trapped into the polymers [38]. There is single stage decomposition for both CNW and their NCEC samples. In particular, the weight loss observed below 200 °C for NCEC thermal degradation curve is due to the loss of $NH_3$ and $CO_2$ successively [39]. The main thermal decomposition profiles for CNW and NCEC samples are explored herein. In short, CNW and NCEC samples started to decompose ($T_0$) mainly at 288 and 276 °C, and the weight loss of 31.9 % and 18.56 % occur at endset ($T_\infty$) 316.77 and 321.6 °C, respectively, which are due to depolymerisation,

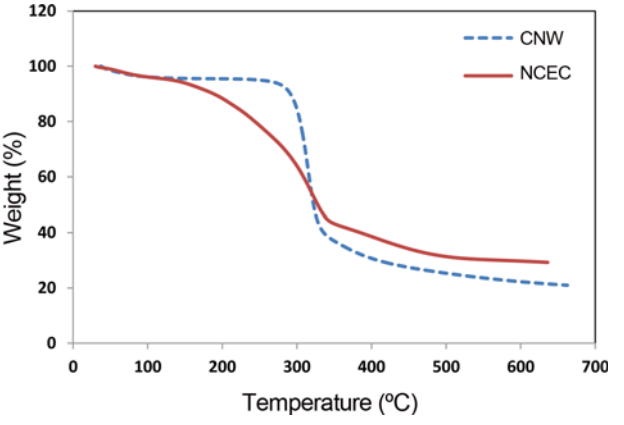


**Figure 5.** TGA analysis curves for CNW and NCEC.

**Table 1.** Weight loss % of CNW and NCEC at temperature of pyrolysis concluded from TGA analysis

| Conc. of sulfuric acid | Evaporation | | Main decomposition | | | | | Residual content (wt%) |
|---|---|---|---|---|---|---|---|---|
| | | | Decomposition temp. | | Remaining weight (%) | | Weight loss (%) | |
| | wt% | Temp. | $T_0$ | $T_\infty$ | $W_0$ | $W_\infty$ | | |
| CNW | 3.87 | 100 | 288.41 | 316.77 | 91.11 | 59.21 | 31.9 | 27.79 |
| NCEC | 3.89 | 100 | 276.84 | 321.6 | 71.8 | 53.24 | 18.56 | 29.34 |

dehydration and decomposition of glycosyl units followed by the formation of a charred residue.

This indicates that NCEC is thermally more stable than CNW, as indicated from the weight loss %, viz, the more weight loss is the less thermal stable. In other words, etherification of CNW with acrylamide leads to enhancement in the thermal stability of the cellulosic material.

**NCEC as Precursor for Green Synthesis of AgNPs**

The silver nanoparticles (AgNPs) were prepared by a simple wet chemical method using soluble NCEC as precursor. Thus, the dual role of NCEC as reducing and stabilizing agent would be understood. NCEC serves as reducing agent through the reducing end groups of the parent CNW chains. On the other hand, stabilization is induced by coordination of amino and carboxylic groups of NCEC with $Ag^+$ so preventing further coalescence and aggregation [40,41]. However, capping of the silver nanocluster with NCEC by virtue of the polymeric nature of the latter and the onset of this on stabilization of AgNPs cannot be ruled out.

The stability and size distribution of nanosilver colloids depend strongly on the relative concentrations of $Ag^+$, reducing agent and the presence of stabilizing agent. Briefly, 1.0 g of NCEC was dissolved in little amount of distilled water followed by addition of 0.3 g NaOH to the solution. After a while, the solution was completed to 100 m*l* and then temperature raised to 70 °C. To this solution, $AgNO_3$ was added drop-wise under stirring for 30 min. The color of medium was observed where it changes gradually to yellowish brown indicating formation of AgNPs. A very intense color is due to plasmon resonance absorption, which can be attributed to the collective oscillation of conduction electrons that is induced by an electromagnetic field [42]. The reduction of silver ions was, routinely, monitored by visual inspection of the solution, as well as, by UV-vis spectra, and TEM.

Influence of $AgNO_3$ concentrations on the reduction efficiency and stability as well as on shape and size of the formed nanosilver colloids was investigated. Interest in preparation of AgNPs colloids, which acquire higher concentrations of the nano-sized silver particles were, therefore, stimulated. Thus different concentrations of $AgNO_3$ were applied to obtain final concentrations of 100, 500, 1000, and 2000 ppm as detailed under.

Figure 6 shows the UV-vis spectra of AgNPs obtained when 1.0 g/100 m*l* NCEC was used as a reducing agent for $Ag^+$ ions and a stabilizing agent for $Ag^o$ atom along with different concentrations of $AgNO_3$. The results bring into focus a number of observations which may be summarized as follows: (a) at low concentration of $AgNO_3$ 100 ppm, the plasmon absorbance band occurs at maximum wavelength 420 nm indicating formation of well stabilized AgNPs successfully. This means that, NCEC is able to reduce and stabilize the $Ag^o$ formed; (b) increasing the concentration of the solution up to 2000 ppm is accompanied by appreciable

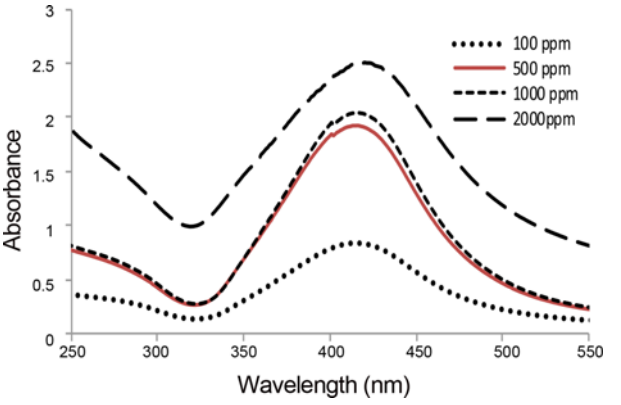


**Figure 6.** UV-vis spectroscopy of silver nanoparticles prepared using 1.0 gm/100 m*l* NCEC at different concentrations of $AgNO_3$.

increase in the electronic absorption spectra; (c) the bands become more stronger and still symmetrical, with a pronounced bell shape at maximum wavelength 420 nm, as well-stabilized AgNPs are formed. The results indicate the powerful reducing and stabilizing abilities of NCEC even at high concentration of $Ag^+$.

To confirm the results obtained from the UV-vis absorption spectroscopy, determination of size and size distribution of AgNPs were performed by recording TEM of the prepared silver colloids.

The particle distribution and the nano-sized structure of AgNPs prepared using different initial $AgNO_3$ concentration together with NCEC were investigated by making use of TEM as shown in Figure 7. The numbers of particles were plotted as a function of different average particle diameters to obtain the histogram in the same Figure. It is clear from Figure 7 that at low concentrations (100 ppm), the colloids bring out small sizes with spherical shape ranged from 5-18 nm with relatively narrow particle size distribution, where the major sizes found between 5-10 nm (Figure 7(A) and 7(B)). With increasing $AgNO_3$ concentration up to 1000 ppm, the resulting particles become bigger and broadly distributed in size. Whereas, the range of particle sizes was 12-30 nm, the majority are about 16-20 nm, respectively (Figure 7(C) and 7(D)). Nonetheless, the colloid dispersion is still stable and well-dispersed up to $AgNO_3$ concentration of 2000 ppm (Figure 7(E) and 7(F)), but certainly is accompanied with increasing the particles size as well as the size distribution become much broader, as seemingly, the sizes are in range of 18-40 nm with the majority around 22-30 nm.

The foregoing results indicate a better efficiency as well as tendency of NCEC to reduce and stabilize AgNPs with small and spherical sizes. The presence of both amide and carboxylic groups on the backbone of NCEC enhances the stability of Ag colloids even at higher concentration of $Ag^+$ ions. One of the main challenges of preparation and application of nanoparticles (i.e. AgNPs) is how to prepare high concentration thereof. Figure 7 made it evident that

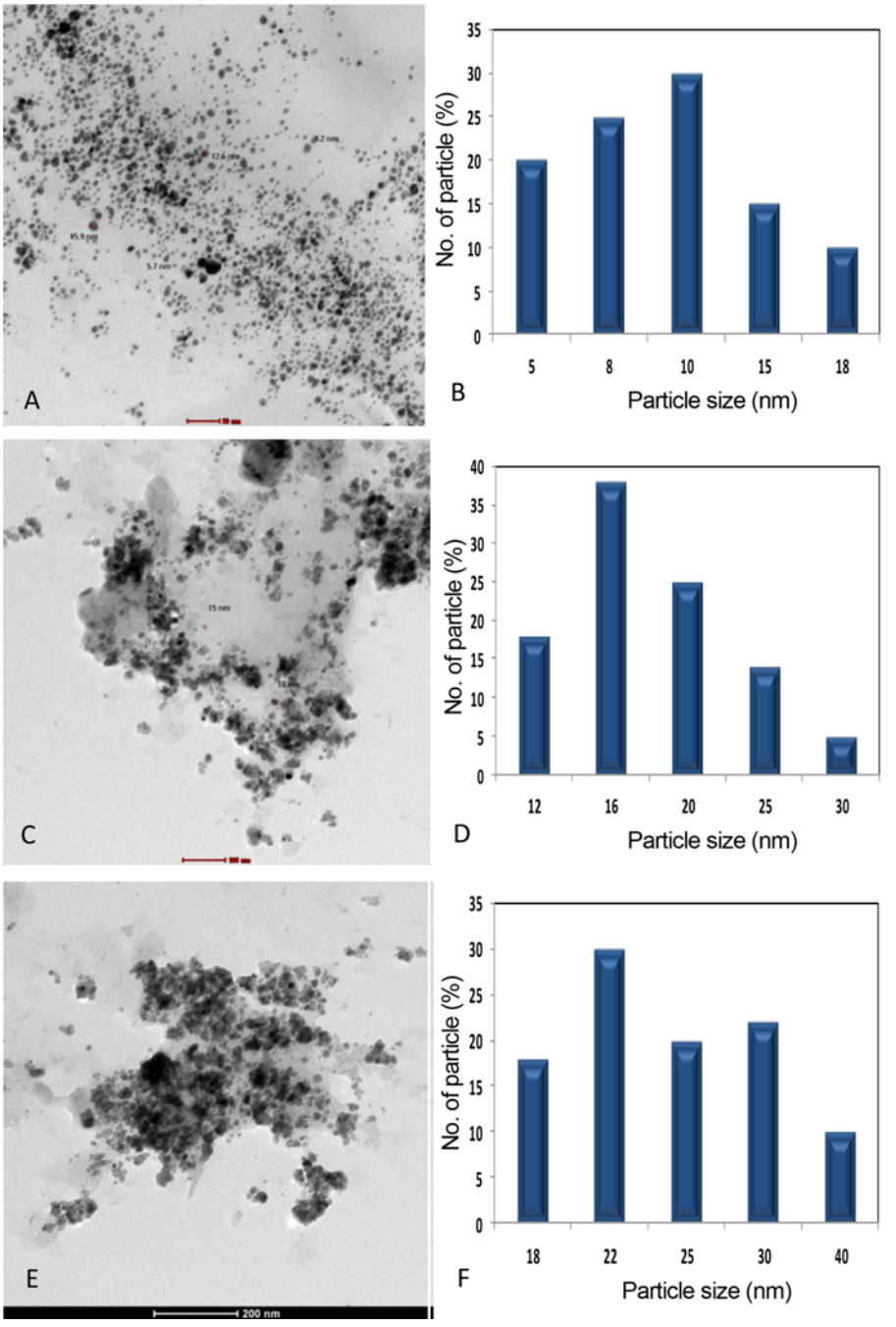


**Figure 7.** TEM micrographs and histograms showing the particle size and particle size distribution of silver nanoparticles prepared using 1.0 gm/100 m*l* NCEC at different concentrations of silver nanoparticles: (A and B) 100 ppm, (C and D) 1000 ppm, and (E and F) 2000 ppm.

1.0 g of NCEC was successfully used to bring about a well-stabilized polydispersed AgNPs with a concentration feasible for industrial applications.

**Synthesis of Electrically Conductive AgNPs-cotton Fabrics Composite**

The dried AgNPs loaded cotton fabrics composite was subjected to further investigations. First, the conductive property of the AgNPs loaded cotton fabric composite was measured and results obtained are shown in Table 2. The weight % of AgNPs in the fabric composite was also monitored using EDX analysis and the results obtained are illustrated in Figure 8 and Table 2.

Obviously, the AgNPs loaded cotton fabric composite

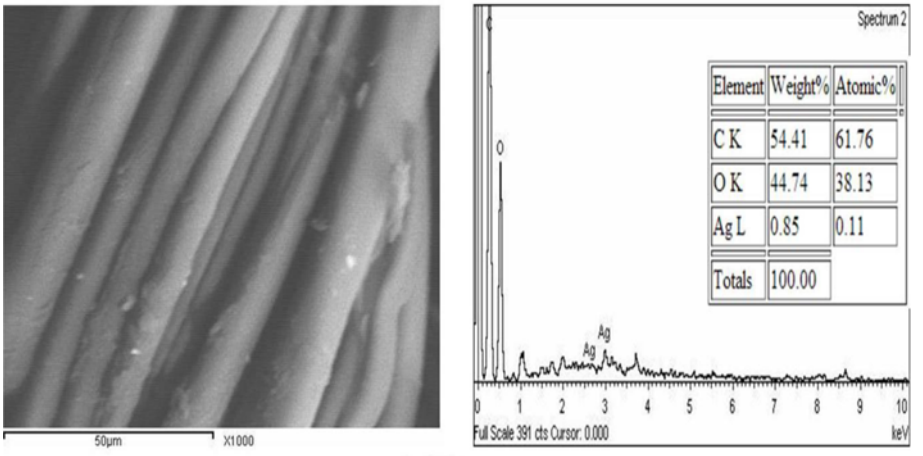


**Figure 8.** SEM image and EDX analysis for AgNPs loaded cotton fabrics composite.

**Table 2.** Conductivity values of AgNPs loaded cotton fabric composite

| Loaded cotton | Conductivity ($\Omega^{-1}\cdot m^{-1}$) | Weight % on the fabrics (EDX) |
|---|---|---|
| Untreated | $5.502\times10^{-10}$ | 0 |
| AgNPs | $1.025\times10^{-7}$ | 0.85 % |

exhibits significant decrease in electrical resistance than blank sample. This decrease in fabric resistance is accompanied by an increase in electrical conductivity of the loaded fabrics. The logical that the conductivity is due to the presence of 8.5 % (w/w) of AgNPs on the fabric as depicted from EDX analysis (Figure 8 and Table 2).

Figure 8 shows the SEM image and EDX analysis of AgNPs loaded cotton fabric composite. The presence of silver nanoparticles could be proved through EDX analysis. From the SEM image, it can also be proved that there is a homogeneous deposition for AgNPs onto the cotton fabric after loading. Furthermore, the protection of fibers against the influence of high-energy electron beam of SEM to which the fibers are exposed implies, the powerful shielding effect of nano-sized carbamoylethyl cellulose film covering the surface of cotton fibers.

For further confirmation, XRD diffraction patterns for AgNPs loaded cotton fabric composite were performed and shown in Figure 9, respectively.

The latter Figure shows, that the XRD pattern of the cotton fibers are coated with silver nanoparticles. Four obvious peaks at $2\theta$=38 °, 44 °, 64 °, and 77 ° correspond to (1 1 1), (2 0 0), (2 2 0), and (3 1 1) crystallographic planes of silver crystal (JCPDS cards 4-0783), respectively. This analysis confirms the face centered cubic (fcc) structure of pure silver crystal. From the XRD patterns, no diffraction peak for other impurities such as $Ag_2O$ was detected. Thus the results confirm that the coating on the cotton fibers is

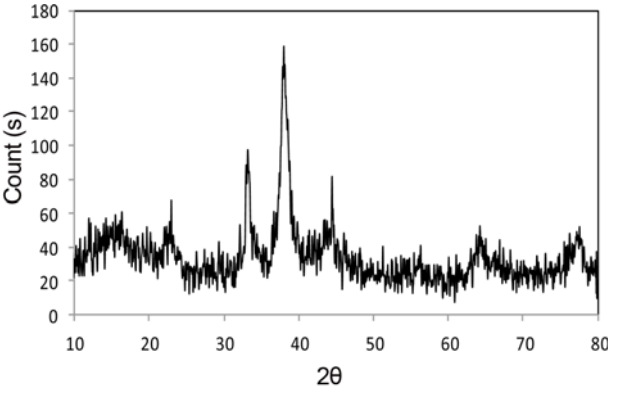


**Figure 9.** XRD pattern of silver nanoparticles loaded onto cotton fabrics prepared using NCEC.

composed of silver crystals only; no other oxides are present; a findings which could be ascribed to the presence of capping agent.

Finally, NCEC as soluble biopolymer is able to produce silver nanoparticles with high concentration which is more feasible for using on industrial scale. In particular, those applications that are concerned with employing of metal nanoparticles as conductive materials for example, functional textiles.

## Conclusion

The main target of the current studies was to develop a new-innovation strategy for synthesis of NCEC and application of the latter in preparation of silver nanoparticles. The innovation is based on conversion of CNW to effective precursors through their carbamoylethylation. Thus NCEC with DS of 0.8 has been prepared successfully via etherification of CNW with acrylamide. FTIR spectra of the NCEC exhibit the existence of new peaks, which confirmed the introduction

of $CH_2$-$CH_2CONH_2$ moieties in the molecular structure of CNW brought about by the carbamoylethylation. XRD patterns and TEM analysis demonstrated that the newly synthesized NCEC has lost its crystalline structure, despite their small size which attained the value of 37.84 nm with a majority of 80.6 % as depicted from DLS analysis. NCEC displayed also higher thermal stability than CNW. In short, carbamoylethylation of CNW resulted in the accomplishment of new product with salient properties. Particularly noteable is the amenability of NCEC to dissolve in hydrophilic solvent.

Being rich in terminal reducing groups in addition to the amide groups, NCEC would certainly function as a strong reducing agent. In combination with this is the polymeric nature of NCEC. Such characteristics would advocate NCEC to serve as stabilizing and reducing agent in the synthesis of nonmetallic particles when AgNPs were prepared as per the chemical reduction method in the presence of NCEC. The well stabilized AgNPs acquired spherical shape even upon using higher concentration of $AgNO_3$ to produce colloidal solution containing AgNPs at concentration of 2000 ppm. The tendency of AgNPs at this latter concentration towards aggregation is limited. As a consequence, AgNPs (1000 ppm) are the most preferable concentration for application in the realm of smart conductive textile.

## References


1. E. Espino-Pérez, J. Bras, V. Ducruet, A. Guinault, A. Dufresne, and S. Domenek, *Eur. Polym. J.,* **49**, 3144 (2013).
2. N. Bitinis, R. Verdejo, J. Bras, E. Fortunati, J. M. Kenny, L. Torre, and M. A. López-Manchado, *Carbohydr. Polym.*, **96**, 611 (2013).
3. K. Missoum, F. Martoïa, M. N. Belgacem, and J. Bras, *Ind. Crop. Prod.*, **48**, 98 (2013).
4. G. Siqueira, J. Bras, and A. Dufresne, *Langmuir*, **26**, 402 (2009).
5. W. Hu, S. Chen, J. Yang, Z. Li, and H. Wang, *Carbohydr. Polym.*, **101**, 1043 (2014).
6. M. M. de Souza Lima and R. Borsali, *Macromol. Rapid Commun.*, **25**, 771 (2004).
7. M. A. S. Azizi Samir, F. Alloin, and A. Dufresne, *Biomacromolecules*, **6**, 612 (2005).
8. H. A. Silvério, W. P. Flauzino Neto, N. O. Dantas, and D. Pasquini, *Ind. Crop Prod.*, **44**, 427 (2013).
9. D. Pasquini, E. D. M. Teixeira, A. A. D. S. Curvelo, M. N. Belgacem, and A. Dufresne, *Ind. Crop Prod.*, **32**, 486 (2010).
10. E. M. Fernandes, R. A. Pires, J. F. Mano, and R. L. Reis, *Prog. Polym. Sci.*, **38**, 1415 (2013).
11. C. Gouss, H. Chanzy, G. Excoffier, L. Soubeyrand, and E. Fleury, *Polymer*, **43**, 2645 (2002).
12. L. Heux, G. Chauve, and C. Bonini, *Langmuir*, **16**, 8210 (2000).
13. J. Araki, M. Wada, and S. Kuga, *Langmuir*, **17**, 21 (2000).
14. V. K. Varshney and S. Naithani in "Cellulose Fibers: Bio- and Nano-Polymer Composites" (S. Kalia, B. S. Kaith, and I. Kaur Eds.), p.43, Springer Berlin, Heidelberg, 2011.
15. J. Ramyadevi, K. Jeyasubramanian, A. Marikani, G. Rajakumar, and A. A. Rahuman, *Mater. Lett.*, **71**, 114 (2012).
16. L. Q. Pham, J. H. Sohn, C. W. Kim, J. H. Park, H. S. Kang, B. C. Lee, and Y. S. Kang, *J. Colloid Interface Sci.*, **365**, 103 (2012).
17. J. P. Ruparelia, A. K. Chatterjee, S. P. Duttagupta, and S. Mukherji, *Acta Biomater.*, **4**, 707 (2008).
18. E. Fortunati, S. Rinaldi, M. Peltzer, N. Bloise, L. Visai, I. Armentano, A. Jiménez, L. Latterini, and J. M. Kenny, *Carbohydr. Polym.*, **101**, 1122 (2014).
19. E. Fortunati, I. Armentano, Q. Zhou, A. Iannoni, E. Saino, L. Visai, L. A. Berglund, and J. M. Kenny, *Carbohydr. Polym.*, **87**, 1596 (2012).
20. N. Drogat, R. Granet, V. Sol, A. Memmi, N. Saad, C. Klein Koerkamp, P. Bressollier, and P. Krausz, *J. Nanopart. Res.*, **13**, 1557 (2011).
21. Y. Shin and G. J. Exarhos, *Mater. Lett.*, **61**, 2594 (2007).
22. Y. Zhou, E.-Y. Ding, and W.-D. Li, *Mater. Lett.*, **61**, 5050 (2007).
23. Y. Shin, I.-T. Bae, B. W. Arey, and G. J. Exarhos, *J. Phys. Chem. C*, **112**, 4844 (2008).
24. H. Liu, D. Wang, S. Shang, and Z. Song, *Carbohydr. Polym.*, **83**, 38 (2011).
25. M. H. El-Rafie, T. I. Shaheen, A. A. Mohamed, and A. Hebeish, *Carbohydr. Polym.*, **90**, 915 (2012).
26. C.-H. Xue, J. Chen, W. Yin, S.-T. Jia, and J.-Z. Ma, *Appl. Surf. Sci.*, **258**, 2468 (2012).
27. A. Hebeish, S. Farag, S. Sharaf, and T. I. Shaheen, *Carbohydr. Polym.*, **102**, 159 (2014).
28. A. Hebeish, S. Farag, S. Sharaf, and T. I. Shaheen, *Cellulose*, **21**, 3055 (2014).
29. A. Vogel, "Elementary Practical Inorganic Chemistry", Longman, London, 1975.
30. V. O. Cirino and S. P. Rowland, *Text. Res. J.*, **46**, 272 (1976).
31. C. S. R. Freire, A. J. D. Silvestre, C. Pascoal Neto, and R. M. A. Rocha, *Cellulose*, **12**, 449 (2005).
32. H. Kang, R. Liu, and Y. Huang, *Polym. Int.*, **62**, 338 (2013).
33. Y. Song, J. Zhou, L. Zhang, and X. Wu, *Carbohydr. Polym.*, **73**, 18 (2008).
34. N. Johar, I. Ahmad, and A. Dufresne, *Ind. Crop. Prod.*, **37**, 93 (2012).
35. K. Z. Hossain, I. Ahmed, A. Parsons, C. Scotchford, G. Walker, W. Thielemans, and C. Rudd, *J. Mater. Sci.*, **47**, 2675 (2012).
36. G. Cheng, P. Varanasi, C. Li, H. Liu, Y. B. Melnichenko, B. A. Simmons, M. S. Kent, and S. Singh, *Biomacromolecules*, **12**, 933 (2011).
37. A. Isogai and R. H. Atalla, *Cellulose*, **5**, 309 (1998).
38. X. Cao, Y. Habibi, and L. A. Lucia, *J. Mater. Chem.*, **19**,

7137 (2009).
39. A. Srivastava, V. Mishra, P. Singh, A. Srivastava, and R. Kumar, *J. Therm. Anal. Calorim.*, **107**, 211 (2012).
40. J. I. Hussain, S. Kumar, A. A. Hashmi, and Z. Khan, *Adv. Mater. Lett.*, **2**, 188 (2011).
41. Y. Zhang, H. Peng, W. Huang, Y. Zhou, X. Zhang, and D. Yan, *J. Phys. Chem. C*, **112**, 2330 (2008).
42. T. Mochochoko, O. S. Oluwafemi, D. N. Jumbam, and S. P. Songca, *Carbohydr. Polym.*, **98**, 290 (2013).